Zero-temperature behavior of the random-anisotropy model in the strong-anisotropy limit

Frauke Liers,[1] Jovanka Lukic,[2] Enzo Marinari,[2] Andrea Pelissetto,[2] and Ettore Vicari[31]

[1] *Institut für Informatik, Pohligstrasse 1, D-50969 Köln, Germany*

[2] *Dipartimento di Fisica dell'Università di Roma "La Sapienza" and INFN, P.le Aldo Moro 2, I-00185 Roma, Italy.*

[3] *Dipartimento di Fisica dell'Università di Pisa and INFN, L.go Pontecorvo 2, I-56100 Pisa, Italy.*

(Dated: July 10, 2007)

Abstract

We consider the random-anisotropy model on the square and on the cubic lattice in the strong-anisotropy limit. We compute exact ground-state configurations, and we use them to determine the stiffness exponent at zero temperature; we find $\theta = -0.275(5)$ and $\theta \approx 0.2$ respectively in two and three dimensions. These results show that the low-temperature phase of the model is the same as that of the usual Ising spin-glass model. We also show that no magnetic order occurs in two dimensions, since the expectation value of the magnetization is zero and spatial correlation functions decay exponentially. In three dimensions our data strongly support the absence of spontaneous magnetization in the infinite-volume limit.

PACS numbers: 75.50.Lk, 05.70.Jk, 75.40.Mg, 77.80.Bh

I. INTRODUCTION

Amorphous alloys of rare earths, such as Dy, and of nonmagnetic transition metals, such as Al, Cu, and Ag, have been extensively studied, both theoretically and experimentally. They are modeled[1] by a Heisenberg model with random uni-axial single-site anisotropy defined on a simple cubic lattice, or, in short, by the random-anisotropy model (RAM)

$$\mathcal{H} = -J \sum_{\langle xy \rangle} \vec{s}_x \cdot \vec{s}_y - D \sum_x (\vec{u}_x \cdot \vec{s}_x)^2, \tag{1}$$

where $\vec{s}_x$ is a three-component spin variable, $\vec{u}_x$ is a unit vector describing the local (spatially uncorrelated) random anisotropy, and D is the anisotropy strength. In amorphous alloys the *a priori* distribution of the quenched vectors $\vec{u}_x$ is usually taken to be isotropic, since, in the absence of crystalline order, there is no preferred direction.

Random anisotropy is a relevant perturbation of the pure Heisenberg model, so that random-anisotropy systems show a critical behavior that is different from the Heisenberg one. Even though the critical behavior of the three-dimensional RAM has been investigated at length in the last thirty years (see Ref. 2 for a review), the phase diagram as a function of D has not yet been determined conclusively. The argument of Imry and Ma for N-vector systems in the presence of a random magnetic field[3] has been extended to the RAM:[4–6] it forbids the existence of a low-temperature phase with non-vanishing magnetization for $d < 4$. An analogous conclusion is obtained by considering the Landau-Ginzburg-Wilson Hamiltonian associated with the RAM:[7,8] no fixed point is found, indicating the absence of a standard magnetic critical transition. However, this does not exclude the possibility of a transition with a low-temperature phase characterized by magnetic quasi-long-range order (QLRO), i.e., a phase in which magnetic correlation functions decay algebraically.[4] Functional renormalization-group calculations[9,10] predict QLRO for small values of D, in agreement with a Landau-Ginzburg calculation of the equation of state for $D \to 0$.[11] In the large-anisotropy limit $D \to \infty$ the model becomes an Ising spin glass, in which the quenched random bond couplings are correlated. If we write $\vec{s}_x = \sigma_x \vec{u}_x$ with $\sigma_x = \pm 1$, the RAM reduces to a particular Ising spin-glass model with Hamiltonian[5]

$$\mathcal{H} = -\sum_{\langle xy \rangle} j_{xy}\, \sigma_x\, \sigma_y\ , \qquad j_{xy} \equiv \vec{u}_x \cdot \vec{u}_y\ , \tag{2}$$

which we call strong random-anisotropy model (SRAM) (We set $J = 1$ without loss of

generality). Model (2) differs from the usual Ising spin-glass model in the bond distribution. Here the random variables j_{xy} on different lattice links are correlated. For instance, one has $\overline{\prod_{\Box} j_{xy}} = 1/27$, where the product is over the links belonging to a given plaquette and the average is taken with respect to the distribution of the vectors $\vec{u}_x$. An interesting hypothesis, originally put forward in Ref. 12, is that in this limit the RAM transition is in the same universality class as that of the Edwards-Anderson Ising spin-glass model (EAM).[13–16] This conjecture was confirmed in two dimensions by a renormalization-group calculation using the large-cell method: the behavior close to the critical point $T = 0$ looks analogous as that of the EAM.[17] In three dimensions instead the phase diagram has been controversial for a long time. While for small values of D numerical simulations[5,18–22] confirmed the existence of a finite-temperature transition (though QLRO was never observed), in the SRAM even the existence of the transition was in doubt.[21] In Ref. 23 a detailed finite-size scaling study provided good evidence for the existence of a finite-temperature glassy transition in the SRAM. Close to the transition, overlap variables, which are the usual order parameters at a spin-glass transition, are critical. The corresponding critical exponents are in good agreement with those obtained for the EAM (see Table 1 in Ref. 24 for a list of recent results) confirming the conjecture of Ref. 12. The transition in the 3D SRAM is not a magnetic transition: magnetic variables are not critical and on both sides of the transition the system is paramagnetic.[23]

It is interesting to note that Hamiltonian (2) is strictly related to that considered by Hopfield[25] in the context of neural networks. The main difference lies in the fact that in the Hopfield model the components of the vectors $\vec{u}_x$ (which are generically N dimensional) are *uncorrelated* equally distributed random variables, while in the SRAM the different components are correlated by the constraint $|\vec{u}_x| = 1$.

The phase diagram of Hamiltonian (2) has been determined in the mean-field approximation in Ref. 26. One finds a critical transition followed by a ferromagnetic phase without spin-glass order. This result, which is quite general and independent of the nature of the distribution of the vectors $\vec{u}_x$,[27–29] (apparently, the precise form of the distribution is only relevant for the type of magnetic order that sets in as the temperature is lowered below the critical point) is in contrast with the arguments of Ref. 4 and the field-theoretical calculations[7,8] and thus does not give us any clue on the low-temperature phase.

In this paper we consider the SRAM in two and three dimensions and study its behavior

at zero temperature. In particular, we determine the stiffness exponent θ, which is related to the finite-size behavior of the domain-wall energy, and several magnetic observables, such as the magnetization, the susceptibility, and the spin-spin second-moment correlation length. For this purpose, by means of an effective exact algorithm,[30,31] we determine an exact ground state for each instance of the randomly chosen vectors $\vec{u}_x$ and for different boundary conditions.

For the stiffness exponent, we find $\theta = -0.275(5)$ in two dimensions and $\theta \approx 0.2$ in three dimensions. These results confirm the conclusions of Refs. 17,23, supporting the existence of a low-temperature glassy phase in three dimensions analogous to that occurring in the EAM and of a two-dimensional zero-temperature glassy transition in the same universality class as the EAM transition with a continuous distribution of the couplings.

As for the magnetic behavior, in two dimensions we can conclude with confidence that there is no magnetic order: the magnetization vanishes and magnetic correlation functions decay exponentially with a very small correlation length, $\xi \approx 2$. In three dimensions we find that the magnetization decreases with system size and that the best fits of the numerical data support the fact that no spontaneous magnetization occurs in the infinite-volume limit. This is in agreement with the results of Ref. 19, in which a similar study was presented and no evidence of magnetic criticality was found. Since in three dimensions our lattices are relatively small (even if they are large as compared to state-of-the-art three-dimensional exact ground-state computations half of the linear extension of the lattice only amounts to five lattice spacings, which, together with the need of taking care of finite-size corrections, does not allow us to distinguish in a clear cut way between a power-law and an exponential decay) we cannot give a final statement about the issue of QLRO, though our data are compatible with an exponential decay of the magnetic correlation functions. As far as we can see, there are no hints that our model is different from a usual EAM in $3D$.

The paper is organized as follows. In Sec. II we define the quantities we compute. In Sec. III we present our numerical results: in Sec. III A we give some details on the numerical methods we use, in Sec. III B we compute the stiffness exponent, while in Sec. III C we discuss the magnetic behavior. Our conclusions are presented in Sec. IV.

II. DEFINITIONS

In this work we focus on the computation of the stiffness exponent θ, of the magnetization of the system and of the magnetic correlation functions. The exponent θ is defined in the following way. We consider a lattice of size L^d and, for each disorder realization, we compute the energies E_P and E_A. The energy E_P is the ground-state energy for the system with periodic boundary conditions, whereas the energy E_A is the ground-state energy for a system in which anti-periodic boundary conditions are used in one direction and periodic boundary conditions in the other $(d-1)$ directions. As usual, anti-periodic boundary conditions are implemented by changing the sign of the bond couplings along one lattice $(d-1)$-dimensional boundary. More precisely, the model with anti-periodic boundary conditions is obtained by considering Hamiltonian (2), *periodic* boundary conditions, and couplings $j_{x_a x_b} = -\vec{u}_{x_a} \cdot \vec{u}_{x_b}$ when $x_a = (1, n_2, \ldots, n_d)$ and $x_b = (L, n_2, \ldots, n_d)$.[32] Then, we define

$$E_m \equiv \overline{E_P - E_A} \qquad\qquad \Delta E = \overline{|E_P - E_A - E_m|}, \tag{3}$$

where the over-line indicates the average over the distribution of the vectors $\vec{u}_x$. Note that in the definition we have subtracted the non-zero average E_m. Only with this subtraction does ΔE provide a measure of the width of the domain-wall distribution. The presence of E_m in the definition deserves some comments. In the usual EAM, $E_m = 0$. Indeed, the bond distribution is invariant under the change of sign of any number of couplings, so that E_A and E_P have the same distribution, which implies $\overline{E}_A = \overline{E}_P$ and therefore $E_m = 0$. Thus, this subtraction is not needed in the EAM definition of ΔE.

In the SRAM, instead, this symmetry does not hold. To understand why we first notice that the products of couplings over closed loops that do not wrap around the lattice (trivial loops) is the same when using periodic or antiperiodic boundary conditions, since in any such loop one always gets an even number of sign changes. Consider now the product $P(n_2, \ldots, n_d) = j_{x_1 x_2} j_{x_2 x_3} \ldots j_{x_L x_1}$, where $x_k = (k, n_2, \ldots, n_d)$, i.e. the product of the bond couplings along one line (which is frequently known as Polyakov line) that wraps around the lattice in the direction where antiperiodic boundary conditions have been imposed. Averaging over the $\{u_x\}$ distribution we obtain

$$\overline{P(n_2, \ldots, n_d)} = 3^{1-L}.$$

When we consider antiperiodic boundary conditions we change the sign of one of the links

belonging to the Polyakov line, and thus in this case the average of $P(n_2, \ldots, n_d)$ is -3^{1-L}. This indicates that the probability distribution of the bond couplings for periodic and antiperiodic boundary conditions is different. Thus, we have $\overline{E}_A \neq \overline{E}_P$, which implies $E_m \neq 0$. Because of that when subtracting E_m, ΔE provides a measure of the width of the domain-wall distribution.

For $L \to \infty$, ΔE behaves as

$$\Delta E \sim L^{\theta}, \tag{4}$$

which defines the exponent θ.

We also consider magnetic correlations. They are defined in terms of the variables $\vec{s}_x = \sigma_x \vec{u}_x$. In particular, we consider the average absolute value of the magnetization per site

$$m = \frac{1}{V} \overline{\left\langle \left| \sum_x \vec{s}_x \right| \right\rangle}, \tag{5}$$

the spin-spin correlation function

$$G(x) \equiv \overline{\langle \vec{s}_0 \cdot \vec{s}_x \rangle} - m^2 = \overline{\vec{u}_0 \cdot \vec{u}_x \langle \sigma_0 \sigma_x \rangle} - m^2, \tag{6}$$

its Fourier transform $\widetilde{G}(p)$, the corresponding susceptibility χ, and the second-moment correlation length ξ:

$$\chi \equiv \sum_x G(x) = \widetilde{G}(0), \tag{7}$$

$$\xi^2 \equiv \frac{1}{4 \sin^2(p_{\min}/2)} \frac{\chi - F}{F}, \qquad F \equiv \widetilde{G}(p) = \sum_x G(x) \cos \frac{2\pi x_1}{L}, \tag{8}$$

where $p = (p_{\min}, 0, 0)$, and $p_{\min} \equiv 2\pi/L$.

III. RESULTS

A. The algorithm

At zero temperature the determination of the thermal averages reduces to the evaluation of the observables in the ground-state configuration. We determine an exact ground state by computing a maximum cut in the interaction graph.[33] This is a prominent problem in combinatorial optimization, which, for general graphs, is NP-hard. However, it can be solved in polynomial time when restricted to two-dimensional lattices with either free boundaries or

$d=2$		$d=3$	
L	$N_0(L)$	L	$N_0(L)$
$L \leq 60$	10000	$L \leq 6$	20000
70	5000	7	14000
80	4000	8	18000
90	4000	9	13860
100	3600	10	4479
110	1600		
120	1000		

TABLE I: Number $N_0(L)$ of computed ground states for two- ($d = 2$) and three-dimensional ($d = 3$) lattices.

periodic boundary conditions where the coupling sizes j_{xy} (assumed integer) are bounded by a polynomial in the size of the input. For the case of continuous couplings that we consider here the complexity status is not known.

For three-dimensional instances, the problem is NP-hard independent of the boundary conditions. For the SRAM model considered here, we use a branch-and-cut approach that is especially designed for solving NP-hard instances.[30,31]

To compute an exact ground state, we consider the lattice as a graph $G = (V, E)$, in which the nodes V are the lattice sites and the edges E are the lattice links that correspond to a non-vanishing coupling (in our case, only nearest neighbors are connected). To each edge we associate a *cost*: the cost $c_{u,v}$ of an edge $(u, v) \in E$ is the negative coupling strength $-j_{uv}$. Given a partition of the nodes into two sets W and $V \setminus W$, we associated to it a cut in G, which is an edge set that contains all edges $e = (u, v)$ such that $u \in W$ and $v \in V \setminus W$. To each cut we associate a *cut value*, which is the sum of the costs of the cut edges. It is not hard to see that a ground state can be obtained as follows. One first determines a maximum cut in G, that is a cut which has a maximal value among all possible cuts. Then, a ground-state spin configuration is obtained by assigning one orientation to the spins that belong to one of the node partitions and the opposite orientation to the others.

To determine a maximum cut, we use a branch-and-cut algorithm from combinatorial optimization. By studying the geometric structure of the problem, we can derive upper

TABLE II: Estimates of θ in two dimensions. We also report the square of the residuals (χ^2) and its value divided by the number of degrees of freedom (DOF).

$L_{\min}$	θ	χ^2	χ^2/DOF
5	$-0.276(2)$	29	1.7
10	$-0.278(3)$	24	2.0
20	$-0.271(4)$	19	1.9
30	$-0.271(7)$	11	1.4
40	$-0.279(9)$	9	1.3

bounds for the maximum-cut value. A lower bound is given by the value of any cut. During the run of the algorithm, we iteratively improve upper and lower bounds on the problem's solution value. It can happen that one cannot improve these bounds any further. In this case we split up the problem into easier sub-problems, which we solve recursively by improving their corresponding upper and lower bounds. We continue the process of tightening the bounds and splitting up the problem into easier sub-problems until upper and lower bounds coincide. This provides an optimal solution and a ground state of the system. Note that in the presence of degeneracies the algorithm finds only one of the ground states. However, since in our case the bond couplings are real numbers, we do not expect degeneracies and thus the algorithm finds the unique ground state.

This exact algorithm allows us to compute the ground state on square lattices L^2, $5 \leq L \leq 120$ and on cubic lattices L^3, $3 \leq L \leq 10$ within reasonable time. For a two-dimensional lattice with $L \leq 80$ and periodic boundary conditions, one ground-state computation takes less than two minutes on average on a SUN Opteron (2.2 GHz) machine; for 120^2 lattices the computation takes 28 minutes. Solving the problem for three-dimensional lattices is more difficult, especially for periodic boundary conditions as we use here. One ground-state computation takes less than 20 seconds for $L \leq 8$, whereas the average CPU time is 8 minutes for $L = 10$. We report the number of computed samples in Table I.

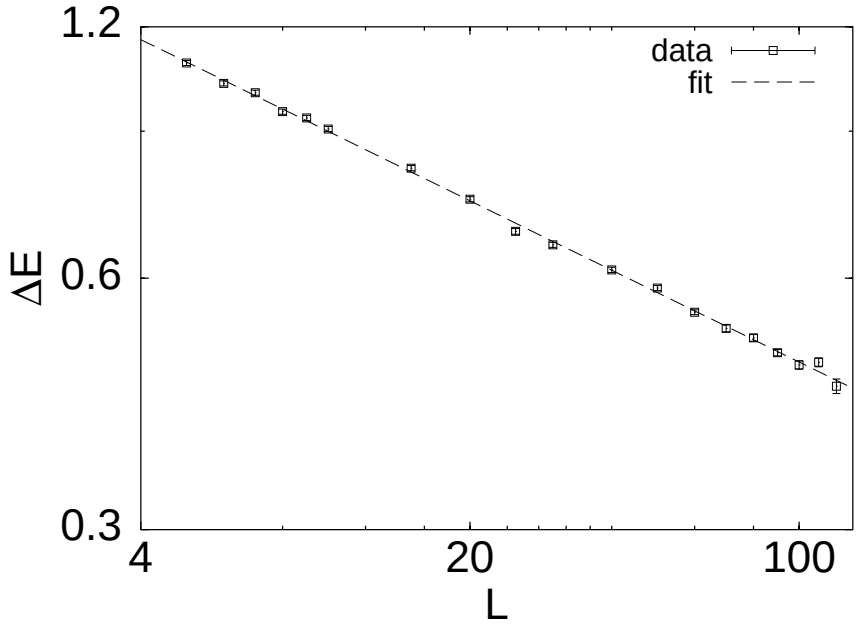

FIG. 1: Estimates of ΔE in two dimensions. We also report the curve aL^θ, $a = 1.699$, $\theta = -0.276$, obtained by fitting all data.

B. Stiffness exponent

We have measured the stiffness exponent in two and in three dimensions. Estimates of ΔE on square lattices L^2, $5 \le L \le 120$ are reported in Fig. 1 versus L. On a logarithmic scale the data fall on a straight line quite precisely. If we fit ΔE to

$$\ln \Delta E = a + \theta \ln L, \tag{9}$$

including only data with $L \ge L_{\rm min}$, we obtain the results reported in Table II. No significant scaling corrections are present and the estimate of θ is constant within error bars. We take as our final estimate

$$\theta = -0.275(5), \tag{10}$$

which includes all results. Estimate (10) should be compared with those obtained for the EAM with continuous energy distributions (if energies are quantized the stiffness exponent vanishes, see the discussion in Ref. 34): $\theta = -0.281(2)$ (Ref. 35), $\theta = -0.282(2)$ (Ref. 36), $\theta = -0.282(3)$ (Ref. 37). Our result is consistent, indicating that the $T = 0$ transition in the SRAM belongs to the same universality class as that of the EAM, as found in Ref. 17.

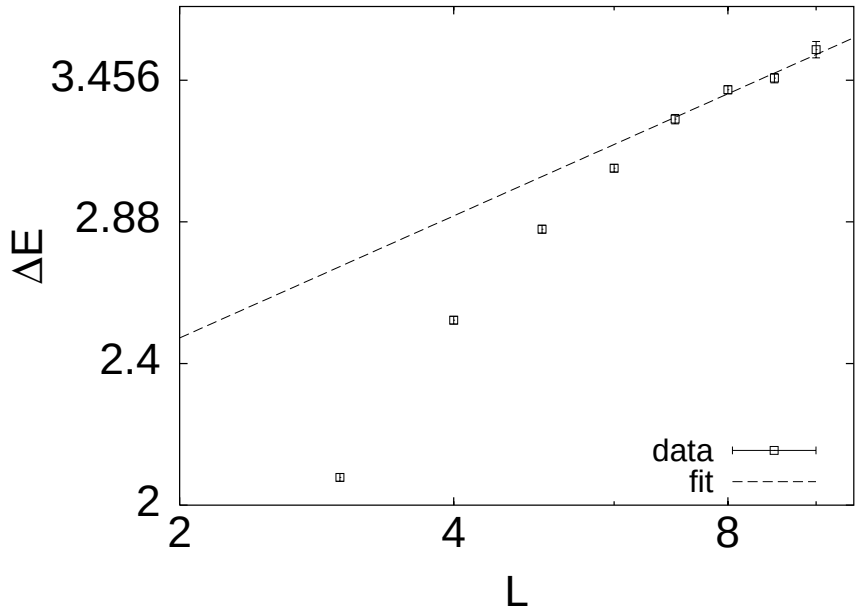

FIG. 2: Estimates of ΔE in three dimensions. We also report the curve aL^θ obtained by fitting the last four data points ($L_{\rm min} = 7$), $a = 2.12$, $\theta = 0.227$.

We have repeated the analysis in three dimensions. Estimates of ΔE on a cubic lattice L^3, $3 \le L \le 10$, are reported in Table III and plotted in Fig. 2. The energy difference ΔE increases with L, indicating that $\theta > 0$. This in turn implies the existence of a low-temperature glassy phase and of a finite-temperature glassy transition, confirming the results of Ref. 23. In order to determine θ we performed fits of the form (9). The results, corresponding to different values of $L_{\rm min}$, are reported in Table IV. In this case there are significant scaling corrections: the χ^2 is large for small values of $L_{\rm min}$ and a significant downward trend is visible in the estimates of θ. A reasonable χ^2 is obtained for $L_{\rm min} \ge 7$, corresponding to $\theta \approx 0.2$. It is difficult to set a reliable error bar on this value. Nonetheless, let us note that this estimate is close to all results obtained for the EAM. A determination of θ on cubic lattices as done here gives $\theta = 0.19(2)$ (Ref. 38) and $\theta \approx 0.19$ (Ref. 37), while the aspect-ratio scaling method gives a slightly different result[37] $\theta \approx 0.27$. Given the uncertainties of the EAM results and the relatively small lattice sizes considered in our investigation, we can certainly conclude that our estimate of θ is fully compatible with the EAM one, confirming the findings of Ref. 23.

TABLE III: Estimates of ΔE, m, χ, and ξ^2 in three dimensions.

L	ΔE	m	χ	ξ^2
3	2.073(10)	0.5601(6)		
4	2.538(13)	0.4985(5)		
5	2.853(15)	0.4468(5)	0.3446(9)	−1.716(3)
6	3.086(15)	0.4022(6)	0.5151(11)	−3.320(7)
7	3.287(20)	0.3638(6)	0.5213(12)	−12.15(7)
8	3.414(18)	0.3292(7)	0.6277(12)	−35.13(3)
9	3.465(21)	0.2986(10)	0.6276(12)	13.82(8)
10	3.595(38)	0.2710(16)	0.6915(24)	12.86(13)

TABLE IV: Estimates of θ in three dimensions. We also report the square of the residuals (χ^2) and its value divided by the number of degrees of freedom (DOF).

$L_{\min}$	θ	χ^2	χ^2/DOF
3	0.465(5)	280	46.7
4	0.390(7)	70	13.9
5	0.338(11)	26	6.4
6	0.294(16)	12	3.9
7	0.227(28)	2.7	1.3
8	0.197(47)	2.1	2.1

C. Magnetic behavior

Once it has been established that the SRAM has a glassy ground state, it is of interest to check whether at $T = 0$ glassy behavior and some kind of magnetic order coexist.

In Fig. 3 we show the average magnetization per site m versus L in two dimensions. The magnetization decreases as expected. Moreover a fit of $\ln m$ to $a + \rho \ln L$ gives $\rho \approx -1$. More precisely, we obtain $\rho = -0.9405(8)$, $-0.9946(17)$, $-1.003(3)$ for $L_{\min} = 5, 10, 20$,

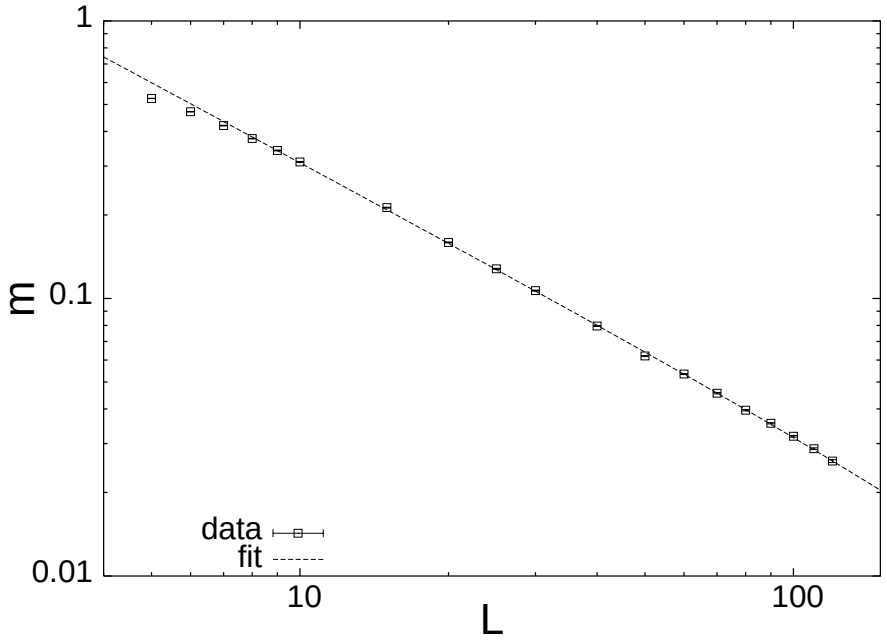

FIG. 3: Estimates of the magnetization m in two dimensions. We also report the curve obtained by fitting all data.

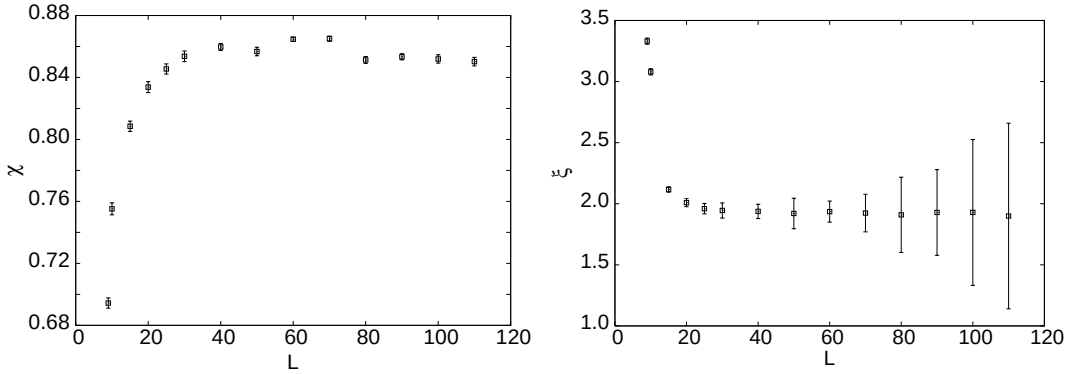

FIG. 4: Estimates of the susceptibility and of the correlation length in two dimensions.

respectively. These results are perfectly consistent with a behavior of the form $m \sim V^{-1/2}$, where V is the volume, which is the expected behavior if the system is paramagnetic. As a check we also computed χ and ξ, which are reported in Fig. 4. They become constant as $L \to \infty$ indicating the absence of magnetic order. Moreover, χ converges to a constant with $1/V$ corrections, as expected: indeed, a fit of χ to $a + b/L^\delta$ gives $a = 0.8617(8), 0.8607(9)$ and $\delta = 2.02(2), 2.18(13)$ for $L_{\rm min} = 5,\ 10$. Analogously, ξ^2 converges to $\xi = 1.90(5)$: magnetic correlations extend only over two lattice spacings. Finally, in Fig. 5 we report

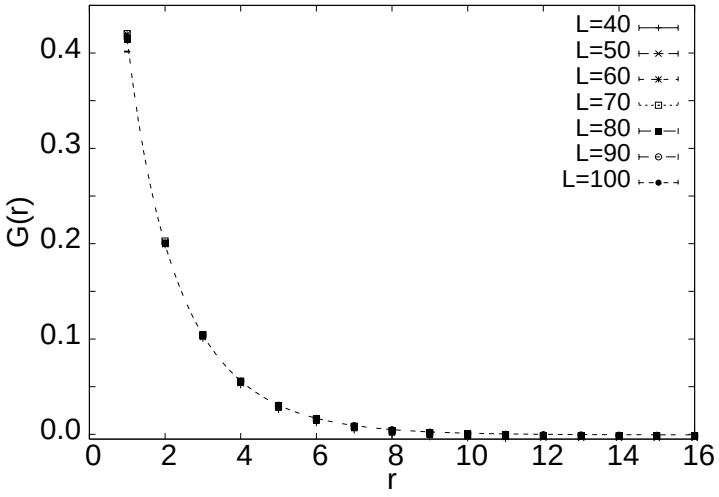

FIG. 5: Connected magnetic correlation function $G(r)$ in two dimensions.

$G(r)$ for several values of L. No L dependence can be observed, so that our data provide the infinite-volume spin-spin correlation function. In two dimensions and in infinite volume we expect

$$G(r) \approx \frac{A}{\sqrt{r}} e^{-r/\xi_e} \tag{11}$$

for $r \to \infty$, where ξ_e is a second definition of correlation length. Fitting the data in the range $r \in [a, b]$, $a \approx$ 3-6, $b \approx$ 13-15, for $L \geq 60$, we always obtain $\xi_e \approx 2$, which is, as expected, close to the estimate of the second-moment correlation length considered before. Clearly, for $T = 0$ the system is not magnetized nor is there QLRO.

Let us now consider the three-dimensional case. The mean values of the magnetization, χ, and ξ^2 are reported in Table III. The magnetization decreases, as already observed in Ref. 19, thus supporting the claim that no spontaneous magnetization occurs. Fits that lead to a non-magnetized infinite-volume limit are always preferred to best fits that imply a spontaneous magnetization: if we fit the data to the form $m + aL^{-x}$, fixing m to a given value (we have tried for example $m = 0.05$, 0.1 and 0.15), the reduced χ^2 decreases with decreasing (fixed) values of m. Also a fit of the correlation functions to an exponential decay has a better χ^2 than a fit to a pure power law (always considering fits with the same number of parameters).

The presence of large finite-size corrections does not allow us to verify the expected asymptotic behavior $m \sim V^{-1/2} \sim L^{-3/2}$. However, as we show in Fig. 6, the data show a clear trend compatible with this behavior. To make a more quantitative comparison we

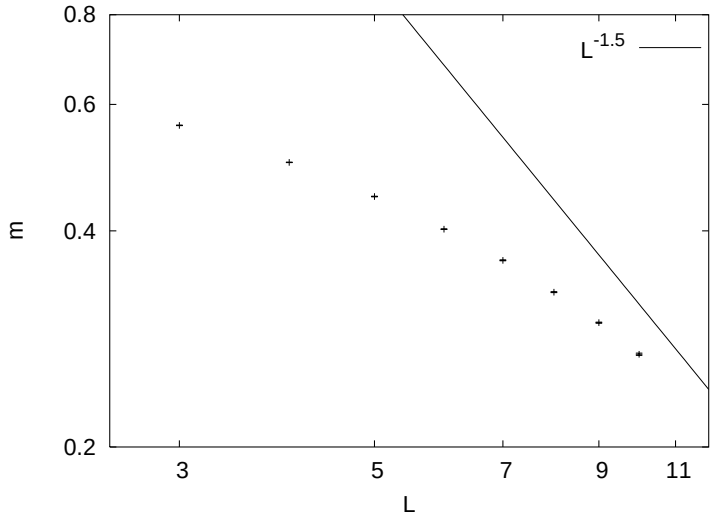

FIG. 6: Log-log plot of the magnetization m in three dimensions as a function of L.

have checked that the deviations can be interpreted as scaling corrections. For this purpose we fit the data with $L \geq 5$ to

$$\frac{A}{L^{1.5}} \left(1 + \frac{B}{L} + \frac{C}{L^2} \right) , \tag{12}$$

including two analytic corrections. If the system is paramagnetic non-analytic exponents are not expected and thus Eq. (12) represents the expected asymptotic form. The fit—the resulting curve is shown in Fig. 7—is quite good and provides very reasonable values for the fit parameters: $A \simeq 15$, $B \simeq -5$, and $C \simeq 8$.

In three dimensions we cannot draw any final conclusion on the question of QLRO from the data of χ and ξ, since currently treatable lattice sizes are too small to allow a clear-cut selection of a given functional behavior. We present here a few comments. First, the values we find for χ are quite small, of the same order of those occurring in two dimensions, where we know with confidence that there is no magnetic critical behavior. Second, note that for $L \leq 8$, ξ^2 is negative. This happens because F [see definition (8)] is small and negative ($F \approx -0.03$ for $L = 8$), indicating that there is no magnetic order, even on a scale of one lattice spacing. For $L = 9, 10$ we find $\xi \approx 3.7$ (the approximate equality of the two values is probably an effect of even-odd oscillations, which are typical of systems with anti-ferromagnetic couplings, and should not be taken as an indication that ξ is already close to its infinite-volume value ξ_∞). Since infinite-volume results can only be obtained if $L \gtrsim c\,\xi$, $c \gtrsim$ 4-5, we expect that lattices with at least $L = 20$ are needed in order to give a definite

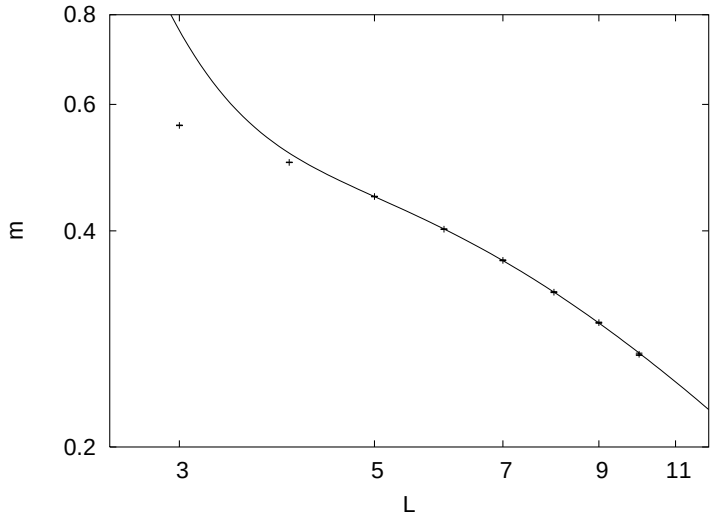

FIG. 7: Three-dimensional average magnetization versus L on a log-log scale. The continuous line is the best fit to (12), which accounts for finite-size corrections (only data with $L \geq 5$ have been considered in the fit).

assessment about the question of magnetic QLRO in three dimensions.

IV. CONCLUSIONS

In this paper we have investigated the behavior of the SRAM at $T = 0$ in two and three dimensions. Our main results are the following:

(i) We determine the stiffness exponent, obtaining $\theta \approx 0.2$ in three dimensions and $\theta = -0.275(5)$ in two dimensions. These results show that the low-temperature behavior of the SRAM is the same as that of the EAM, confirming the conclusions of Refs. 17,23. In particular, the correlation among the bond couplings is irrelevant.

(ii) We investigate the question of the magnetic order. In two dimensions we find no evidence of critical behavior: magnetic correlations die out after a few lattice spacings. In three dimensions we exclude the presence of spontaneous magnetization, in agreement with Ref. 19. The question of QLRO is still open; the limited linear size only allows us to claim that the decay of correlation functions is compatible with an exponential decay. Note that if QLRO would hold at $T = 0$, a second transition should occur, at temperatures below the temperature T_g of the glassy transition found in Ref. 23.

Indeed, the numerical data of Ref. 23 indicate paramagnetic behavior all around T_g.

There are several generalizations of the SRAM that can be investigated with the method we use here. For instance, we could consider N-dimensional vectors u_x with $N \neq 3$ or different distributions of the vectors u_x. In the first case, we can give precise predictions. The correlation of the bond variables around a lattice plaquette becomes $\overline{\prod_{\Box} j_{xy}} = 1/N^3$, which implies that bond correlations vanish for $N \to \infty$. Thus, for $N = \infty$, the SRAM is just an EAM with a different continuous bond distribution. In this limit, therefore, the two models belong to the same universality class. Our results for $N = 3$ imply that the same holds for any $N \geq 3$. For $N = 1$ it is enough to redefine $\sigma_i \to u_i \sigma_i$ to re-obtain the standard ferromagnetic Ising model. The behavior for $N = 2$ is not predicted by our results, since, for $N = 2$, the model is less frustrated than that with $N = 3$ studied here. In three dimensions, numerical studies[19,39–41] provide some evidence that the $N = 2$ SRAM has a magnetic transition with a diverging magnetic susceptibility. The nature of the low-temperature phase is however still controversial.

Little is known for generic distributions of the vector u_x. The arguments of Refs. 4,5 do not necessarily apply to this case. Indeed, they either assume that correlation functions have a Goldstone-like singularity or that the relevant magnetic modes are spin waves. Both assumptions may not hold for generic distributions, since the $O(N)$ symmetry is broken even after averaging over disorder. The only available results are those of Ref. 8 that considers generic cubic-symmetric distributions in three dimensions. They generically exclude the presence of a ferromagnetic transition belonging to the random-exchange universality class (there are some exceptions, but they appear to be of limited practical interest[42]). Different types of magnetic transitions are however still possible, and in this case nothing is known on a possible glassy transition and on the presence of QLRO.

Acknowledgments

We thank Silvio Franz for an interesting conversation. The computations were performed on the Cliot cluster of the Regional Computing Center and on the scale cluster of E. Speckenmeyer's group, both at the University of Köln, Germany. F.L. has been supported by the German Science Foundation (DFG) in the projects Ju 204/9 and Li 1675/1 and by the

Marie Curie RTN ADONET 504438 funded by the EU.

---

[1] R. Harris, M. Plischke, and M. J. Zuckermann, Phys. Rev. Lett. **31**, 160 (1973); R. W. Cochrane, R. Harris, and M. J. Zuckermann, Phys. Rep. **48**, 160 (1973).

[2] M. Dudka, R. Folk, and Yu. Holovatch, J. Magn. Magn. Mater. **294**, 305 (2005). [cond-mat/0406692].

[3] Y. Imry and S.-k. Ma, Phys. Rev. Lett. **35**, 1399 (1975).

[4] R.A. Pelcovits, E. Pytte, and J. Rudnick, Phys. Rev. Lett. **40**, 476 (1978); Erratum **48**, 1297 (1982).

[5] C. Jayaprakash and S. Kirkpatrick, Phys. Rev. B **21**, 4072 (1980).

[6] A. Brooks Harris, R. G. Caflisch, and J. R. Banavar, Phys. Rev. B **35**, 4929 (1987).

[7] M. Dudka, R. Folk, and Yu. Holovatch, Cond. Matt. Phys. **4**, 77 (2001); M. Dudka, R. Folk, and Yu. Holovatch, in *Fluctuating Paths and Fields*, edited by W. Janke, A. Pelster, H.-J. Schmidt, and M. Bachmann (World Scientific, Singapore, 2001) [cond-mat/0106334].

[8] P. Calabrese, A. Pelissetto, and E. Vicari, Phys. Rev. E **70**, 036104 (2004) [cond-mat/0311576];

[9] D. E. Feldman, Phys. Rev. B **61**, 382 (2000).

[10] D. E. Feldman, Int. J. Mod. Phys. B **15**, 2945 (2001)[cond-mat/0201243].

[11] A. Aharony and E. Pytte, Phys. Rev. Lett. **45**, 1583 (1980); Phys. Rev. B **27**, 5872 (1983).

[12] J. H. Chen and T. C. Lubensky, Phys. Rev. B **16**, 2106 (1977).

[13] S.F. Edwards and P. W. Anderson, J. Phys. F **5**, 965 (1975).

[14] M. Mézard, G. Parisi, and M. A. Virasoro, *Spin-Glass Theory and Beyond* (World Scientific, Singapore, 1987).

[15] K. H. Fischer and J. A. Hertz, *Spin Glasses* (Cambridge University Press, Cambridge UK, 1991).

[16] N. Kawashima and H. Rieger, Recent progress in spin glasses in *Frustrated Spin Systems*, edited by H. T. Diep (World Scientific, Singapore, 2004) [cond-mat/0312432].

[17] A. J. Bray and M. A. Moore, J. Phys. C: Solid State **18**, L139 (1985).

[18] A. Chakrabarti, Phys. Rev. B **36**, 5747 (1987).

[19] R. Fisch, Phys. Rev. B **42**, 540 (1990).

[20] R. Fisch, Phys. Rev. B **58**, 5684 (1998) [cond-mat/9801033].

[21] M. Itakura, Phys. Rev. B **68**, 100405(R) (2003) [cond-mat/0303552].

[22] O. V. Billoni, S. A. Cannas, and F. A. Tamarit, Phys. Rev. B **72**, 104407 (2005).

[23] F. Parisen Toldin, A. Pelissetto, and E. Vicari, J. Stat. Mech.: Theory Expt. P06002 (2006).

[24] H. Katzgraber, M. Körner, and A. P. Young, Phys. Rev. B **73**, 224432 (2006) [cond-mat/0602212].

[25] J. Hopfield, Proc. Natl. Acad. Sci. USA **79**, 2554 (1982); *ibid.* B **1**, 3088 (1984).

[26] B. Derrida and J. Vanneminus, J. Phys. C: Solid State **13**, 3261 (1980).

[27] K. H. Fischer and A. Zippelius, J. Phys. C: Solid State **18**, L1139 (1985).

[28] D. J. Amit, H. Gutfreund, and H. Sompolinsky, Phys. Rev. A **32**, 1007 (1985).

[29] J. P. Provost and G. Vallee, Phys. Rev. Lett. **50**, 598 (1983).

[30] F. Liers, M. M. Jünger, G. Reinelt, and G. Rinaldi, in *New Optimization Algorithms in Physics*, edited by A. K. Hartmann and H. Rieger (Wiley-VCH, Berlin, 2004), p. 47.

[31] F. Barahona, M. Grötschel, M. Jünger, and G. Reinelt, Operations Research **36**, 493 (1988).

[32] We could impose antiperiodic boundary conditions directly on model (1), i.e., set $\vec{s}_{L+1,\dots} = -\vec{s}_{1,\dots}$ and $\vec{u}_{L+1,\dots} = -\vec{u}_{1,\dots}$. This amounts to consider model (1) with interaction $+J\vec{s}_{x_a} \cdot \vec{s}_{x_b}$, when $x_a = (1, \dots, n_d)$ and $x_b = (L, \dots, n_d)$. Under the mapping $\vec{s}_x = \vec{u}_x \sigma_x$, we reobtain the same Hamiltonian discussed in the text.

[33] F. Barahona, J. Phys. A: Math. Gen. **15**, 3241 (1982).

[34] C. Amoruso, E. Marinari, O. C. Martin, and A. Pagnani, Phys. Rev. Lett. **91**, 087201 (2003).

[35] H. Rieger, L. Santen, U. Blasum, M. Diehl, M. Jünger, and G. Rinaldi, J. Phys. A **29**, 3939 (1996); (erratum) J. Phys. A **30**, 8795 (1997).

[36] A. K. Hartmann and A. P. Young, Phys. Rev. B **64**, 180404 (2001).

[37] A. C. Carter, A. J. Bray, and M. A. Moore, Phys. Rev. Lett. **88**, 077201 (2002).

[38] A. K. Hartmann, Phys. Rev. E **59**, 84 (1999).

[39] R. Fisch and A. B. Harris, Phys. Rev. B **41**, 11305 (1990).

[40] R. Fisch, Phys. Rev. Lett. **66**, 2041 (1991).

[41] R. Fisch, Phys. Rev. B **51**, 11507 (1995).

[42] In some particular cases, when disorder preserves the reflection symmetry $s_{x,a} \to -s_{x,a}$, $s_{x,b} \to s_{x,b}$ for any pair $b \neq a$ (this is, for example, realized when the probability distribution vanishes outside the lattice axes), there is a standard order-disorder transition with a low-temperature magnetized phase. Continuous transitions in these models belong to the same universality class

as that of the random-exchange Ising model, see D. Mukamel and G. Grinstein, Phys. Rev. B **25**, 381 (1982), Ref. 8, and Yu. Holovatch, V. Blavats'ka, M. Dudka M, C. von Ferber, R. Folk, and T. Yavors'kii, Int. J. Mod. Phys. B **16**, 4027 (2003) [cond-mat/0111158].